

Resonance Production

Patricia Fachini §

Brookhaven National Laboratory, Upton, NY, 11973, USA

Abstract. Recent results on $\rho(770)^0$, $K(892)^*0$, $f_0(980)$, $\phi(1020)$, $\Delta(1232)^{++}$, and $\Lambda(1520)$ production in A+A and $p + p$ collisions at SPS and RHIC energies are presented. These resonances are measured via their hadronic decay channels and used as a sensitive tool to examine the collision dynamics in the hadronic medium through their decay and regeneration. The modification of resonance mass, width, and shape due to phase space and dynamical effects are discussed.

PACS numbers: 25.75.Dw,13.85.Hd

1. Introduction

The in-medium modification of vector mesons has been proposed as a possible signal of a phase transition of nuclear matter to a deconfined plasma of quarks and gluons in relativistic heavy-ion collisions [1].

Even in the absence of a phase transition, at normal nuclear density, the modification of vector meson properties are expected to be measurable. Effects such as phase space [2, 3, 4, 5, 6, 7, 8, 9, 10] and dynamical interactions with matter [4, 6, 8, 11] may modify the resonance mass, width, and shape. These modifications of the vector meson properties take place close to kinetic freeze-out, in a dilute hadronic gas at late stages of heavy-ion collisions. At such low matter density, the proposed modifications are expected to be small, but observable. The effects of phase space due to the rescattering of hadrons and Bose-Einstein correlations between the daughters from the resonance decay and the hadrons in the surrounding matter are present in $p + p$ [3, 4, 6, 10] and Au+Au [2, 4, 5, 6, 7, 8, 9, 11] collisions. The interference between different pion scattering channels can effectively distort the line shape of resonances [12]. Dynamical effects due to vector mesons interacting with the surrounding matter are also expected to be present in both systems, and have been evaluated for the latter [4, 6, 8, 11].

Those resonances that decay before kinetic freeze-out may not be reconstructed due to the rescattering of the daughter particles. In this case, the resonance survival probability is relevant and depends on the time between chemical and kinetic freeze-outs, the source size, and the p_T of the resonance. On the other hand, after chemical freeze-out, elastic interactions may increase the resonance population compensating for

§ To whom correspondence should be addressed (pfachini@bnl.gov)

the ones that decay before kinetic freeze-out. This resonance regeneration depends on the hadronic cross-section of their daughters. For example, the K^* regeneration depends on the $K\pi$ cross section (σ) while the rescattering of the daughter particles depends on $\sigma_{\pi\pi}$ and $\sigma_{\pi p}$, which are considerably larger (factor ~ 5) than $\sigma_{K\pi}$ [13, 14, 15]. In the case of the Δ^{++} , the regeneration probability is expected to be higher than the rescattering of the daughters since $\sigma_{\pi p} > \sigma_{\pi\pi}$ [13, 15]. Thus, the study of resonances can provide an independent probe of the time evolution of the source from chemical to kinetic freeze-outs and yield detailed information on hadronic interaction at later stages.

2. Results

The $\rho(770)^0$ [16, 17], $K(892)^{*0}$ [17], $f_0(980)$ [18], $\phi(1020)$ [19], $\Delta(1232)^{++}$ [17], $\Lambda(1520)$ [20], and $\Sigma(1385)$ [20, 21] production were measured via their hadronic decay channels at midrapidity ($|y| \leq 0.5$) in Au+Au and $p + p$ collisions at $\sqrt{s_{NN}} = 200$ GeV using the STAR detector at RHIC. The ϕ [22] meson was also studied via its hadronic decay channel at $|y| \leq 0.5$ in Au+Au collisions using the PHENIX detector at RHIC. At SPS, the ϕ [23] meson was recently measured via its hadronic decay channel by NA49 at $0.0 \leq y \leq 2.0$ for the top 7% of the inelastic hadronic Pb+Pb cross-section at $E_{beam} = 80, 40, 30,$ and 20 AGeV ($\sqrt{s_{NN}} = 12.32, 8.76, 7.62,$ and 6.27 GeV, respectively).

The ρ^0 mass is shown as a function of p_T in Fig. 1 for peripheral Au+Au (40-80% of the inelastic hadronic cross-section), high multiplicity $p + p$ (top 10% of the minimum bias $p + p$ multiplicity distribution for $|\eta| < 0.5$), and minimum bias $p + p$ interactions. The ρ^0 mass was obtained by fitting the data to a p -wave Breit-Wigner function times the phase space (BW \times PS) described in [16]. Figure 1 also depicts the Δ^{++} mass and width as a function of charged particle multiplicity ($dN_{ch}/d\eta$) for minimum bias $p + p$ and Au+Au collisions. The Δ^{++} mass was obtained by fitting the data to the BW \times PS function [16] and a gaussian function representing the residual background described in [17]. Figure 2 also shows the K^{*0} mass and width as a function of p_T for central Au+Au (top 10% of the hadronic cross-section) and minimum bias $p + p$ interactions. The K^{*0} mass was obtained by fitting the data to the BW \times PS function [16] and a linear function representing the residual background described in [17].

The Δ^{++} mass measured in minimum bias $p + p$ and Au+Au collisions for low values of $dN_{ch}/d\eta$ is lower than the value reported in [15] within statistical errors even after correcting for phase space (PS). Both mass and width increase as a function of centrality, and while the Δ^{++} mass is in agreement with the value reported in [15] for large values of $dN_{ch}/d\eta$ within statistical errors, its width is larger than the average reported in [15]. The increase of the Δ^{++} mass as a function of centrality was predicted in a recent calculation that introduces the in-medium modification of the Δ^{++} [4]. Both ρ^0 and K^{*0} masses increase as a function of p_T and are systematically lower than the value reported in [15]. The K^{*0} width is in agreement with the average presented in [15]. The ρ^0 mass measured in peripheral Au+Au collisions is lower than the minimum bias $p + p$ measurement. The mass for high multiplicity $p + p$ interactions is lower

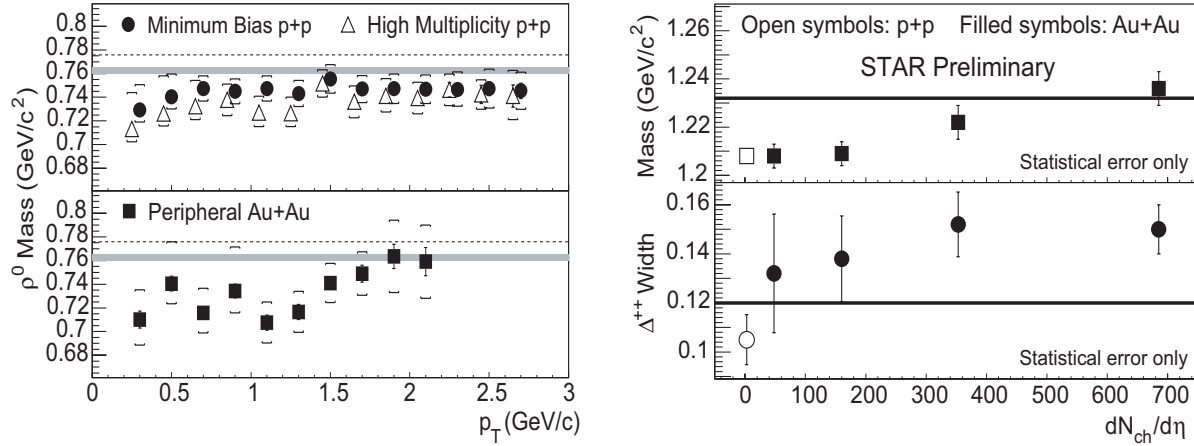


Figure 1. Left panel: The ρ^0 mass as a function of p_T . The error bars indicate the systematic uncertainty. The dashed lines represent the average of the ρ^0 mass measured in e^+e^- [15]. The shaded areas indicate the ρ^0 mass measured in $p + p$ collisions [24]. The open triangles have been shifted downward on the abscissa for clarity. Right panel: Δ^{++} mass (top) and width (bottom) as a function of $dN_{ch}/d\eta$. The solid lines correspond to the average of the Δ^{++} mass and width reported in [15]. The errors shown are statistical only.

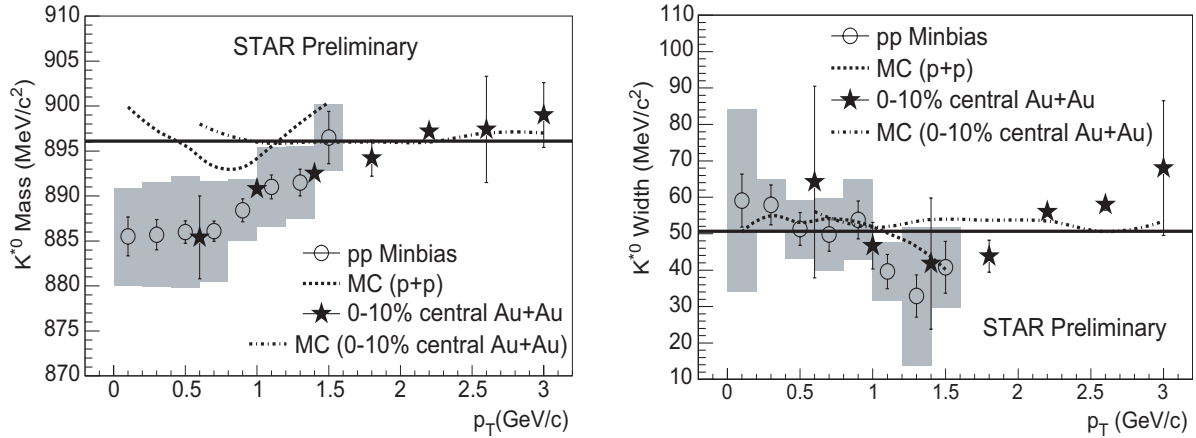


Figure 2. The K^{*0} mass (left panel) and width (right panel) as a function of p_T . The grey shaded boxes are the systematic uncertainties in minimum bias $p + p$. The solid lines correspond to the average of the K^{*0} mass and width reported in [15]. The dotted and dashed lines are the results from the Monte Carlo simulations, which accounts for detector effects and kinematic cuts, for the Au+Au and $p + p$ measurements, respectively. The errors shown for the Au+Au measurement are statistical only.

than for minimum bias $p + p$ interactions for all p_T bins, indicating that the ρ^0 mass is also multiplicity dependent. Recent calculations are not able to reproduce the ρ^0 mass measured in peripheral Au+Au collisions without introducing in-medium modification of the ρ^0 meson [4, 5, 6, 7, 8, 9, 11].

Previous observations of the ρ meson in e^+e^- [24, 25, 26] and $p + p$ interactions [27] indicate that the ρ^0 line shape is considerably distorted from a p -wave Breit-Wigner

function. A mass shift of $-30 \text{ MeV}/c^2$ or larger was observed in e^+e^- collisions at $\sqrt{s} = 90 \text{ GeV}$ [24, 25, 26]. In the $p + p$ measurement at $\sqrt{s} = 27.5 \text{ GeV}$ [27], a ρ^0 mass of $0.7626 \pm 0.0026 \text{ GeV}/c^2$ was obtained from a fit to a relativistic p -wave Breit-Wigner function times the phase space [27]. This result is the only $p + p$ measurement used in the hadro-produced ρ^0 mass average reported in [15].

The ρ^0 [16, 17] and f_0 [18] measurements do not have sufficient sensitivity to permit a systematic study of their widths and the mass of the later. The ϕ [19, 22, 23] and the $\Lambda(1520)$ [17] masses and widths are in agreement with the values reported in [15].

The ρ^0/π ratios as a function of c.m. system energy are depicted in Fig. 3. The ρ^0/π ratios are from measurements in e^+e^- [28, 29, 30], $p + p$ [27, 31, 32, 33], K^+p [34], and π^-p [35] interactions at different c.m. system energies compared to the recent STAR measurement at $|y| < 0.5$ for minimum bias $p + p$ and peripheral Au+Au collisions [16, 17] at $\sqrt{s_{NN}} = 200 \text{ GeV}$. The Δ^{++}/p ratios from measurements in e^+e^- [36], $p + p$ [27], $p + \text{Pb}$ [37], and $\text{Pb} + \text{Pb}$ [38] interactions are also shown in Fig. 3 and compared to the recent STAR measurement at $|y| < 0.5$ for minimum bias $p + p$ and for the top 5% of the inelastic hadronic Au+Au cross-section [17] at $\sqrt{s_{NN}} = 200 \text{ GeV}$. Figure 4 depicts the ϕ/K^- ratios as a function of $\sqrt{s_{NN}}$. The ratios are from measurements in Au+Au collisions at 4.87 GeV [39] and in Pb+Pb collisions for the top 5% of the inelastic hadronic cross-section at 17.27 GeV [40], which are compared to the recent NA49 results for the top 7% of the inelastic hadronic Pb+Pb cross-section at $\sqrt{s_{NN}} = 12.32, 8.76, 7.62, \text{ and } 6.27 \text{ GeV}$ [23], the recent STAR measurements at $|y| < 0.5$ for minimum bias $p + p$ and for the top 10% of the inelastic hadronic Au+Au cross-section at $\sqrt{s_{NN}} = 200 \text{ GeV}$ [19], and the recent PHENIX measurement at $|y| < 0.5$ for the top 10% of the inelastic hadronic Au+Au cross-section at $\sqrt{s_{NN}} = 200 \text{ GeV}$ [22]. For the top 10% of the inelastic hadronic Au+Au cross-section at $\sqrt{s_{NN}} = 200 \text{ GeV}$, while the ϕ inverse slope obtained from STAR [19] and PHENIX [22] are in agreement, there is a factor of 2 difference in the normalization that corresponds to a 1.25σ effect. The difference in the ϕ measurement between STAR and PHENIX is under investigation. The K^{*0}/K ratios from measurements in e^+e^- [28, 29, 30, 41], $p + p$ [27, 33, 42], and $\bar{p} + p$ [43] interactions at different c.m. system energies are also shown in Fig. 4 and compared to the recent STAR measurement at $|y| < 0.5$ for minimum bias $p + p$ and for the top 10% of the inelastic hadronic Au+Au cross-section at $\sqrt{s_{NN}} = 200 \text{ GeV}$ [17]. The STAR measurements of the ϕ/K^- and K^{*0}/K^- ratios at $|y| < 0.5$ for the top 10% of the inelastic hadronic Au+Au cross-section at $\sqrt{s_{NN}} = 130 \text{ GeV}$ [44, 45] are also depicted in Fig. 4.

The ρ^0/π , K^{*0}/K , ϕ/K^- , and Δ^{++}/p ratios shown in Fig. 3 and Fig. 4 do not present a strong dependence on the colliding system or the c.m. system energy, with the exception of the K^{*0}/K^- ratio at $\sqrt{s_{NN}} = 200 \text{ GeV}$. In this case, the K^{*0}/K^- ratio for the top 10% of the inelastic hadronic Au+Au cross-section is lower than the minimum bias $p + p$ measurement at the same c.m. system energy by a factor of 2.

Figure 5 depicts the ρ^0/π^- , K^{*0}/K^- , f_0/π^- , ϕ/K^- , Δ^{++}/p , and Λ^*/Λ ratios as a function of $dN_{ch}/d\eta$ at $\sqrt{s_{NN}} = 200 \text{ GeV}$ measured by STAR. All ratios have been

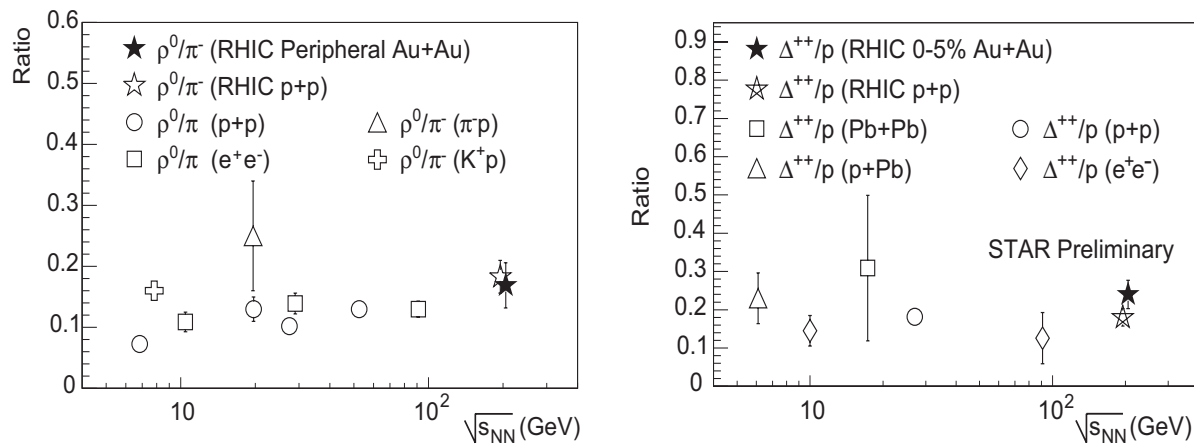


Figure 3. Left: ρ^0/π ratios in e^+e^- [28, 29, 30], $p+p$ [27, 31, 32, 33], K^+p [34], and π^-p [35] interactions at different c.m. system energies compared to the recent STAR measurement at $|y| < 0.5$ for minimum bias $p+p$ and peripheral Au+Au collisions at $\sqrt{s_{NN}} = 200$ GeV [16, 17]. Right: Δ^{++}/p ratios in e^+e^- [36], $p+p$ [27], $p+Pb$ [37], and $Pb+Pb$ [38] interactions at different c.m. system energies compared to the recent STAR measurement at $|y| < 0.5$ for minimum bias $p+p$ and for the top 5% of the inelastic hadronic Au+Au cross-section at $\sqrt{s_{NN}} = 200$ GeV [17]. The errors on the ratios at $\sqrt{s_{NN}} = 200$ GeV are the quadratic sum of the statistical and systematic errors. The ratios at $\sqrt{s_{NN}} = 200$ GeV are offset from one another for clarity.

normalized to the corresponding ratio measured in minimum bias $p+p$ collisions at the same $\sqrt{s_{NN}}$ and indicated by the dashed line in Fig. 5. As mentioned previously and shown in Fig. 4, the K^{*0}/K^- ratio for the top 10% of the inelastic hadronic Au+Au cross-section is lower than the minimum bias $p+p$ measurement at the same c.m. system energy by a factor of 2. In addition, statistical model calculations [6, 7, 46] are considerably larger than the measurement presented in Fig. 5. The K^{*0} regeneration depends on $\sigma_{K\pi}$ while the rescattering of the daughter particles depends on $\sigma_{\pi\pi}$ and $\sigma_{\pi p}$, which are considerably larger (factor ~ 5) than $\sigma_{K\pi}$ [13]. The lower K^{*0}/K^- ratio measured may be due to the rescattering of the K^{*0} decay products. The ρ^0/π^- and f_0/π^- ratios from minimum bias $p+p$ and peripheral Au+Au interactions at the same c.m. system energy are comparable. Statistical model calculations [6, 7, 46] for Au+Au collisions underpredict considerably the ρ^0/π^- and f_0/π^- ratios presented in Fig. 5. The larger ρ^0/π^- ratio measured may be due to the interplay between the rescattering of the ρ^0 decay products and ρ^0 regeneration. The rescattering of the ϕ decay products and the ϕ regeneration should be negligible due to the ϕ longer lifetime (~ 44 fm/c) and the small σ_{KK} , respectively. As a result, statistical model calculations [7, 46] reproduce the ϕ/K^- ratio measurement depicted in Fig. 5. The centrality dependence of the ϕ/K^- ratio disfavors the kaon coalescence production mechanism for ϕ mesons. Rescattering models [47] predict an increase in the ϕ/K^- ratio as a function of centrality; however, the measurement does not support such behavior, as can be observed in Fig. 5. The Δ^{++}/p ratio depicted in Fig. 5 has the opposite behavior than the K^{*0}/K^- ratio. While the K^{*0}/K^- ratio decreases from minimum bias $p+p$ to Au+Au interactions, the Δ^{++}/p

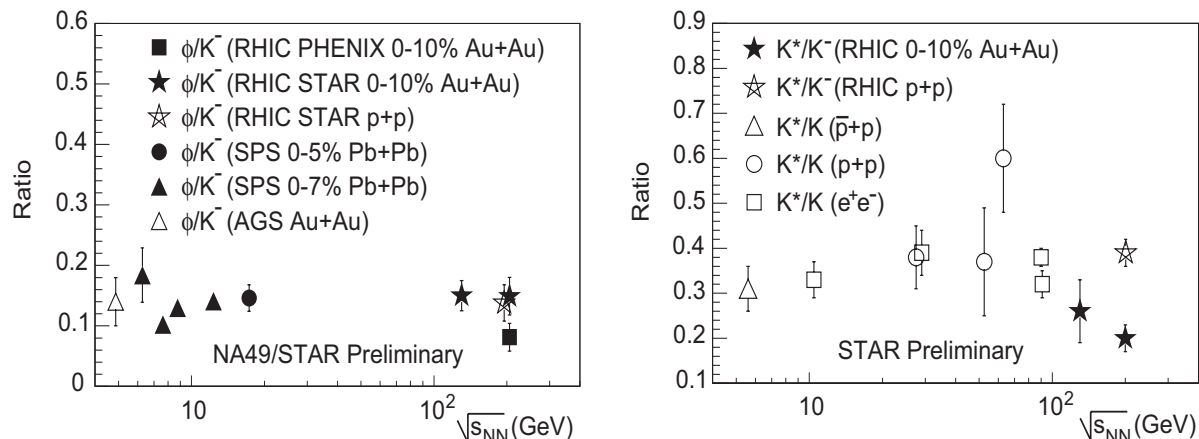


Figure 4. Left: ϕ/K^- ratios in Au+Au collisions at 4.87 GeV [39] and in Pb+Pb collisions for the top 5% of the inelastic hadronic cross-section at 17.27 GeV [40] compared to the recent NA49 results for the top 7% of the inelastic hadronic Pb+Pb cross-section at $\sqrt{s_{NN}} = 12.32, 8.76, 7.62,$ and 6.27 GeV [23], the recent STAR measurements at $|y| < 0.5$ for minimum bias $p+p$ and for the top 10% of the inelastic hadronic Au+Au cross-section at $\sqrt{s_{NN}} = 200$ GeV [19], and the recent PHENIX measurement at $|y| < 0.5$ for the top 10% of the inelastic hadronic Au+Au cross-section at $\sqrt{s_{NN}} = 200$ GeV [22]. The ϕ/K^- ratios at $\sqrt{s_{NN}} = 200$ GeV are offset from one another for clarity. Right: K^*/K^- ratios in e^+e^- [28, 29, 30, 41], $p+p$ [27, 33, 42], and $\bar{p}+p$ [43] interactions at different c.m. system energies compared to the recent STAR measurement at $|y| < 0.5$ for minimum bias $p+p$ and for the top 10% of the inelastic hadronic Au+Au cross-section at $\sqrt{s_{NN}} = 200$ GeV [17]. The STAR measurements of the ϕ/K^- and K^*/K^- ratios at $|y| < 0.5$ for the top 10% of the inelastic hadronic Au+Au cross-section at $\sqrt{s_{NN}} = 130$ GeV [44, 45] are also depicted. The errors on the ratios at $\sqrt{s_{NN}} = 200$ GeV are the quadratic sum of the statistical and systematic errors.

ratio remains constant, or even slightly increase from minimum bias $p+p$ to central Au+Au interactions. In the case of the Δ^{++} , the regeneration probability should be higher than the rescattering of the decay products since $\sigma_{\pi p} > \sigma_{\pi\pi}$ [13, 15]. Statistical model calculations [7, 46] for Au+Au collisions underpredicts the Δ^{++}/p ratio presented in Fig. 5. The larger Δ^{++}/p ratio measured may be due to the interplay between the rescattering of the Δ^{++} decay products and Δ^{++} regeneration.

The centrality dependence of the resonance ratios depicted in Fig. 5 suggests that the ϕ regeneration and the rescattering of the ϕ decay products are negligible, and the Δ^{++} regeneration is slightly larger than the rescattering of the Δ^{++} decay products. In addition, the results shown in Fig. 5 also suggest that the rescattering of the K^{*0} decay products is dominant over the K^{*0} regeneration and therefore the reaction channel $K^* \leftrightarrow K\pi$ is not in balance. As a result, the K^{*0}/K^- ratio can be used to estimate the time between chemical and kinetic freeze-outs. Assuming that the minimum bias $p+p$ measurement corresponds to the production at chemical freeze-out and using the most central measurement of the K^{*0}/K^- ratio in Au+Au collisions for the production at kinetic freeze-out, the time between chemical and kinetic freeze-outs is short (~ 3 fm/c).

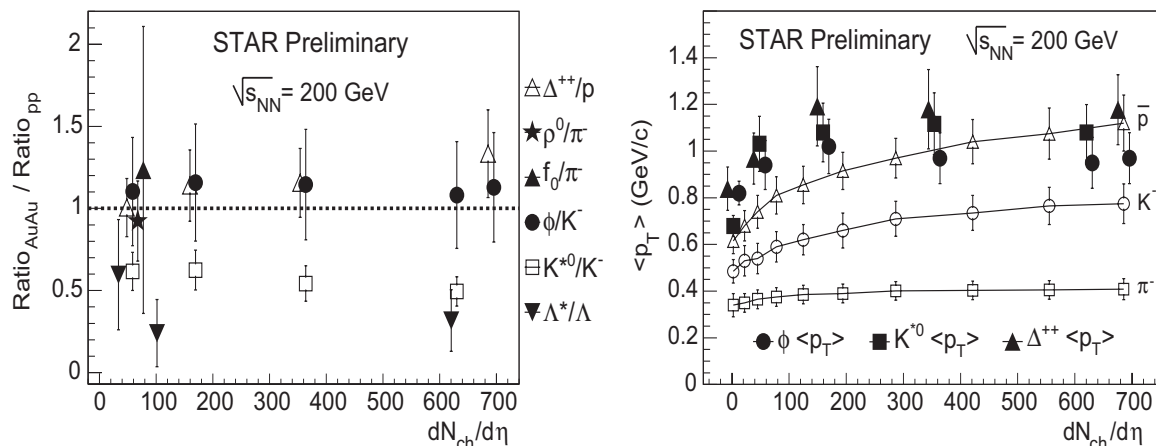


Figure 5. Left panel: The ρ^0/π^- , K^{*0}/K^- , f_0/π^- , ϕ/K^- , Δ^{++}/p , and Λ^*/Λ ratios as a function of $dN_{ch}/d\eta$ at $\sqrt{s_{NN}}=200$ GeV measured by STAR. All ratios have been normalized to the corresponding ratio measured in minimum bias $p+p$ collisions at the same c.m. system energy and indicated by the dashed line. Right panel: The K^{*0} , ϕ , and Δ^{++} $\langle p_T \rangle$ as a function of $dN_{ch}/d\eta$ compared to that of π^- , K^- , and \bar{p} . The errors shown are the quadratic sum of the statistical and systematic errors.

The K^{*0} , ϕ , and Δ^{++} average transverse momentum ($\langle p_T \rangle$) as a function of $dN_{ch}/d\eta$ are compared to that of π^- , K^- , and \bar{p} in Fig. 5. The K^{*0} , ϕ , and Δ^{++} $\langle p_T \rangle$ do not present a significant centrality dependence. This is contrary to the general behavior of π^- , K^- , and \bar{p} $\langle p_T \rangle$ that increase as a function of $dN_{ch}/d\eta$, as expected if the transverse radial flow of these particles increases.

3. Conclusions

Recent results on resonance production in A+A and $p+p$ collisions at SPS and RHIC energies were presented. The measured ρ^0 , K^{*0} , and Δ^{++} masses are lower than previous measurements reported in [15] while the Δ^{++} width is larger than the average reported in [15]. Dynamical interactions with the surrounding matter, interference between various scattering channels, phase space distortions, and Bose-Einstein correlations are possible explanations for the apparent modification of resonance properties. The centrality dependence of resonance ratios may be interpreted in the context of hadronic cross sections. Using the K^{*0}/K^- ratio, the time between chemical and kinetic freeze-outs was estimated to be short (~ 3 fm/c). Further studies of resonances can provide important information on the dynamics of relativistic collisions and help in understanding the properties of nuclear matter under extreme conditions.

Acknowledgements

The author would like to thank M. Bleicher, P. Braun-Munzinger, W. Broniowski, G.E. Brown, W. Florkowski, P. Kolb, G.D. Lafferty, F. Laue, R. Longacre, S. Pratt, R. Rapp, E. Shuryak, T. Ullrich, Z. Xu, and H. Zhang for valuable discussions.

References

- [1] Rapp R and Wambach J 2000 *Adv. Nucl. Phys.* **25** 1.
- [2] Barz H W *et al.* 1991 *Phys. Lett. B* **265** 219.
- [3] P. Braun-Munzinger, Private communication.
- [4] Shuryak E V and Brown G E 2003 *Nucl. Phys. A* **717** 322.
- [5] Kolb P F and Prakash M 2003 *Preprint* nucl-th/0301007.
- [6] Rapp R 2003 *Nucl. Phys. A* **725** 254.
- [7] Broniowski W *et al.* 2003 *Preprint* nucl-th/0306034.
- [8] Bleicher M and Stöcker H 2004 *J. Phys. G* **30** S111.
- [9] Pratt S and Bauer W 2003 *Preprint* nucl-th/0308087.
- [10] Granet P *et al.* 1978 *Nucl. Phys. B* **140** 389.
- [11] Ayala A *et al.* 2004 *Preprint* hep-ph/0403220.
- [12] Longacre R S 2003 *Preprint* nucl-th/0303068.
- [13] Protopopescu S D *et al.* 1973 *Phys. Rev. D* **7** 1279.
- [14] Matison M J *et al.* 1974 *Phys. Rev. D* **9** 1872.
- [15] Hagiwara K *et al.* 2002 *Phys. Rev. D* **66** 010001.
- [16] Adams J *et al.* 2003 *Preprint* nucl-ex/0305034.
- [17] Zhang H 2004 *J. Phys. G* **30** S577; *Preprint* nucl-ex/0403010.
- [18] Fachini P 2004 *J. Phys. G* **30** S565.
- [19] Ma J 2004 *J. Phys. G* **30** S543.
- [20] Markert C 2004 These proceedings.
- [21] Salur S 2004 *Preprint* nucl-ex/0403009.
- [22] Seto R 2004 These proceedings.
- [23] Gazdzicki M 2004 These proceedings.
- [24] Acton P D *et al.* 1992 *Z. Phys. C* **56** 521; Lafferty G D 1993 *Z. Phys. C* **60** 659.
- [25] Ackerstaff K *et al.* 1998 *Eur. Phys. J. C* **5** 411.
- [26] Buskulic D *et al.* 1996 *Z. Phys. C* **69** 379.
- [27] Aguilar-Benitez M *et al.* 1991 *Z. Phys. C* **50** 405.
- [28] Albrecht H *et al.* 1994 *Z. Phys. C* **61** 1.
- [29] Derrick M *et al.* 1985 *Phys. Lett. B* **158** 519.
- [30] Pei Y J *et al.* 1996 *Z. Phys. C* **72** 39.
- [31] Blobel V *et al.* 1974 *Phys. Lett. B* **48** 73.
- [32] Singer R *et al.* 1976 *Phys. Lett. B* **60** 385.
- [33] Drijard D *et al.* 1981 *Z. Phys. C* **9** 293.
- [34] Chliapnikov P V *et al.* 1980 *Nucl. Phys. B* **176** 303.
- [35] Winkelmann F C *et al.* 1975 *Phys. Lett. B* **56** 101.
- [36] Chun S and Buchanan C 1998 *Phys. Rep.* **292** 239.
- [37] Barish K N *et al.* 2003 *Phys. Rev. C* **67** 014902.
- [38] Aggarwal M M *et al.* 2000 *Phys. Lett. B* **477** 37.
- [39] Back B B *et al.* 2003 *Preprint* nucl-ex/0304017.
- [40] Afanasiev S V *et al.* 2000 *Phys. Lett. B* **491** 59.
- [41] Abe K *et al.* 1999 *Phys. Rev. D* **59** 052001.
- [42] Akesson T *et al.* 1982 *Nucl. Phys. B* **203** 27.
- [43] Canter J *et al.* 1979 *Phys. Rev. D* **20** 1029.
- [44] Adler C *et al.* 2002 *Phys. Rev. C* **65** 041901(R).
- [45] Adler C *et al.* 2002 *Phys. Rev. C* **66** 061901(R).
- [46] Braun-Munzinger P *et al.* 2001 *Phys. Lett. B* **518** 41; Stachel J and Magestro D, Private communication.
- [47] Bleicher M *et al.* H 1999 *J. Phys. G* **25** 1854;